Physica A 392 (2013) 1439–1451

Contents lists available at SciVerse ScienceDirect

Physica A

journal homepage: www.elsevier.com/locate/physa

Efficiency and probabilistic properties of bridge volatility estimator

S. Lapinova [a], A. Saichev [b,*], M. Tarakanova [b]

[a] National Research University Higher School of Economics, Russia
[b] Nizhni Novgorod State University, Russia

ARTICLE INFO

Article history:
Received 24 March 2012
Received in revised form 9 November 2012
Available online 27 November 2012

Keywords:
Volatility estimators
Probabilistic properties
Efficiency
Unbiasedness

ABSTRACT

We discuss the efficiency of the quadratic bridge volatility estimator in comparison with Parkinson, Garman–Klass and Roger–Satchell estimators. It is shown in particular that point and interval estimations of volatility, resting on the bridge estimator, are considerably more efficient than analogous estimations, resting on the Parkinson, Garman–Klass and Roger–Satchell ones.

1. Introduction

Volatility, defined as the variance of the increments of the log-price over a specific time interval, is a universally used risk indicator. Most of the existing high-frequency variance estimators are modifications of the well-known realized volatility (see, for instance, Refs. [1–3]), and are based on the knowledge of the open and close prices of n time-step intervals dividing the whole time interval of interest.

With the growing availability of high-frequency tick-by-tick price time series, a number of new efficient volatility estimators have been developed (see, for instance, Refs. [4–6]). We present here a comparative analysis of the efficiency of the quadratic bridge volatility estimator [7] and the well-known Parkinson (PARK) [8], Garman–Klass (GK) [9] and Roger–Satchell (RS) [10,11] volatility estimators, based on high and low values of the log-price increments within given time intervals. Some fruitful information and detailed analysis of stochastic price models and efficiency of high–low-close volatility estimators one can find in the recent article Ref. [12]. Detailed and valuable discussion of stochastic volatility models and volatility estimators, related to the topic of the present paper, are provided in G. Ramey and V. Ramey Ref. [13] and in Bonanno et al. Refs. [14,15].

We show that the high–low quadratic bridge estimator, discussed in this work, is significantly more efficient, for the point and interval volatility estimations, than the above-mentioned PARK, GK and RS estimators, at least in the framework of the geometric Brownian motion with a drift model of the price stochastic process. Notice that some related results concerning statistical properties of volatility estimators were obtained in Saichev et al. Ref. [16], where they have discussed constructions of most efficient volatility estimators. It was shown that efficiencies of the pointed out most efficient estimators are very close to the efficiency of the quadratic bridge estimator discussed in this paper. From another side, the shortcoming of the most efficient estimators, discussed in Ref. [16], is that they have much more complicated structure than the quadratic bridge estimator, discussed in this paper.

For the Brownian motion model of log-price process, the advantage of the quadratic bridge estimator can be intuitively understood as follows. It is well-known that the high and low values of a Brownian motion process are most probably found

* Correspondence to: Bodenacherstrasse 67, 8121, Benglen, Switzerland. Tel.: +41 44577050541.
E-mail address: saichev@hotmail.com (A. Saichev).

0378-4371/$ – see front matter © 2012 Elsevier B.V. All rights reserved.
doi:10.1016/j.physa.2012.11.047

in the neighborhood of the edges of the observation interval. In contrast, by construction of the bridge, its high and low values are in general distant from the edges (see Fig. B.1 at the end of the article, where are depicted distributions of instants of high value occurrence for the Brownian motion and the corresponding bridge). As a result, the high and low of a bridge incorporate significantly more information about the variability of the original stochastic process than its own high and low values.

It is worthwhile to stress additionally that one cannot calculate intraday volatility, due to the lack of historical financial markets data, during the middle (and even at the end) of the previous century. But now there are accessible even tick-by-tick price data for most financial markets and stocks. So, one can now easily calculate values of the intraday bridge high–low volatility estimators.

Notice in conclusion that it seems at first glance that high-frequency (or even tick-by-tick) realized-volatility estimators might be more efficient than any high–low estimators. It is, of course, right in the framework of the geometrical Brownian motion model of the price stochastic behavior. Unfortunately, the mentioned model failed at the small time scales. Moreover, there is a microstructure noise effect, making high-frequency realized-volatility estimators biased and less efficient even in the case of zero drift. Concerning quantitative description of the microstructure noise effect see our paper [17] and the references therein.

The paper is organized as follows. In Section 2 a short description of high–low volatility estimators, including the quadratic bridge estimator, suggested in this work, is given. In Section 3, the statistical description of high–low volatility estimators, in the framework of the Brownian motion model of the log-price stochastic process, is discussed in detail. In Section 4, we compare the efficiency of PARK and quadratic bridge estimators. In Section 5, we give a comparative probabilistic analysis of the interval estimations, resting on the bridge, PARK, GK and RS volatility estimators. In Section 6 the results of statistical testing of the above-mentioned volatility estimators are described. In Section 7 we draw the conclusions.

2. Examples of volatility estimators

Consider the dependence on time t of the price $P(t)$ of some financial instrument. As a rule, in discussing volatility, one consider its logarithm

$$X(t) := \ln P(t).$$

Let us point out one of the conventional volatility $V(T)$ definitions, which we are using in this work. It is the variance

$$V(T) := \mathbf{Var}[Y(t,T)] = \mathbf{E}[Y^2(t,T)] - \mathbf{E}^2[Y(t,T)]$$

of the log-price increment $Y(t,T) := X(t+T) - X(t)$ within a given time interval duration T.

Recall that GK [9], PARK [8] and RS [10] volatility estimators are resting on the high and low values:

$$H := \sup_{t'\in(0,T)} Y(t,t'), \qquad L := \inf_{t'\in(0,T)} Y(t,t').$$

Accordingly, the PARK estimator is equal to

$$\hat{V}_p := (H-L)^2/\ln 16, \tag{1}$$

while the GK estimator is given by the expression

$$\begin{aligned} &\hat{V}_g := k_1(H-L)^2 - k_2(C(H+L) - 2HL) - k_3C^2, \\ &k_1 = 0.511, \qquad k_2 = 0.0109, \qquad k_3 = 0.383. \end{aligned} \tag{2}$$

Here $C := Y(t,T)$ is the close value of the log-price increment. Recall also the RS estimator, equal to

$$\hat{V}_r := H(H-C) + L(L-C).$$

Besides the mentioned well-known estimators, we discuss the quadratic bridge estimator. Below we call it briefly the *bridge estimator*. Before we define it, recall the definition of the bridge $Z(t,t')$ of stochastic process $Y(t,t')$. It is equal to

$$Z(t,t') := Y(t,t') - \frac{t'}{T}Y(t,T), \quad t' \in (0,T). \tag{3}$$

Let introduce the high and low of the bridge:

$$\mathcal{H} := \max_{t'\in(0,T)} Z(t,t'), \qquad \mathcal{L} := \min_{t'\in(0,T)} Z(t,t').$$

Accordingly, the bridge volatility estimator mentioned above is given by

$$\hat{V}_b := \kappa(\mathcal{H} - \mathcal{L})^2. \tag{4}$$

The value of the factor κ will be calculated later on.

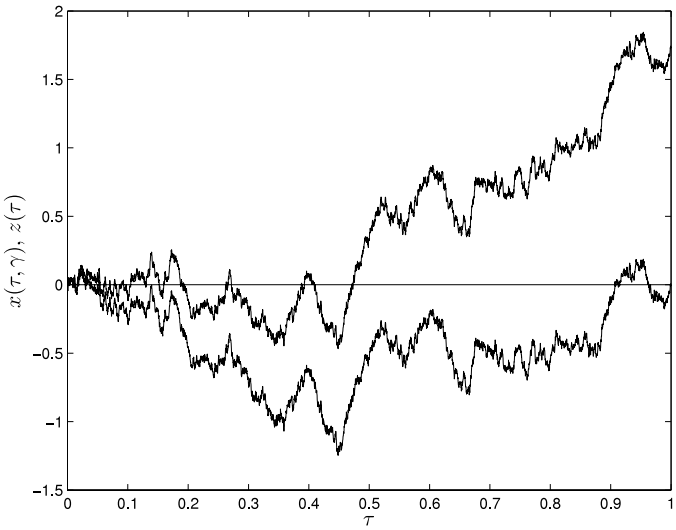

Fig. 1. Typical paths of canonical Brownian motion $x(\tau,\gamma)$ (5) for $\gamma = 1$ and corresponding canonical bridge $z(\tau)$ (9).

3. Geometric Brownian motion

One of the conventional models of price stochastic behavior is geometric Brownian motion (see Refs. [18–20]). In particular, it is used in theoretical justification of GK, PARK and RS estimators. Below we discuss statistics of the mentioned volatility estimators in the framework of the geometric Brownian motion model. Namely, we assume that the increment of the log-price is of the form

$$Y(t,T) = \mu T + \sigma B(T).$$

Here μ is the drift of the price, while $B(t)$ is the standard Brownian motion $B(t) \sim \mathcal{N}(0,t)$. The factor σ^2 is the intensity of the Brownian motion. Using the well-known Brownian motion self-similar property, one can ensure that

$$\begin{aligned} &Y(t,t') \sim \sigma\sqrt{T}x(\tau,\gamma), \\ &x(\tau,\gamma) := \gamma\tau + B(\tau), \qquad \gamma := \mu\sqrt{T}/\sigma, \qquad \tau := t'/T \in (0,1). \end{aligned} \tag{5}$$

Henceforth we call process $x(\tau,\gamma)$ by *canonical Brownian motion*, while the factor γ by *canonical drift*. Using relations (1), (2), and (4) and (5), one finds that

$$\begin{aligned} &\hat{V}_p \sim V(T)\cdot\hat{v}_p(\gamma), \qquad \hat{V}_g \sim V(T)\cdot\hat{v}_g(\gamma), \qquad \hat{V}_b \sim V(T)\cdot\hat{v}_b, \\ &\hat{V}_r \sim V(T)\cdot\hat{v}_r(\gamma), \quad V(T) = \sigma^2 T. \end{aligned}$$

We have used the above *canonical estimators*:

$$\begin{aligned} &\hat{v}_p(\gamma) := \mathrm{d}^2/\ln 16, \qquad \hat{v}_b := \kappa s^2, \qquad \mathrm{d} := h - l, \qquad s := \xi - \zeta, \\ &\hat{v}_g(\gamma) := k_1\mathrm{d}^2 - k_2(c\mathrm{d} - 2hc) - k_3c^2, \qquad \hat{v}_r = h(h-c) + l(l-c), \end{aligned} \tag{6}$$

containing high, low and close values

$$h := \sup_{\tau\in(0,1)} x(\tau,\gamma), \qquad l := \inf_{\tau\in(0,1)} x(\tau,\gamma), \qquad c := x(1,\gamma), \tag{7}$$

of canonical Brownian motion, and high and low values

$$\xi := \sup_{\tau\in(0,1)} z(\tau), \qquad \zeta := \inf_{\tau\in(0,1)} z(\tau), \tag{8}$$

of the canonical bridge

$$z(\tau) := x(\tau,\gamma) - \tau x(1,\gamma) = B(\tau) - \tau\cdot B(1), \quad \tau \in (0,1). \tag{9}$$

Plots of the typical paths of the canonical Brownian motion $x(\tau,\gamma)$ (5) for $\gamma = 1$ and corresponding canonical bridge $z(\tau)$ (9) are given in Fig. 1.

It is worthwhile to note that the closer the expected values of canonical estimators $\hat{v}_p(\gamma)$, $\hat{v}_g(\gamma)$, $\hat{v}_r$ and $\hat{v}_b$ are to unity, the less biased are the corresponding original volatility estimators. Analogously, the smaller the variances of canonical estimators the more efficient the original volatility estimators $\hat{V}_p$, $\hat{V}_g$, $\hat{V}_r$ and $\hat{V}_b$.

Notice additionally that canonical drift γ of the canonical Brownian motion $x(\tau,\gamma)$ (5) is, as a rule, unknown. Nevertheless, to get some idea about dependence on drift μ of bias and efficiency of volatility estimators, we will discuss below in detail the dependence of canonical estimator statistical properties on possible values of the factor γ.

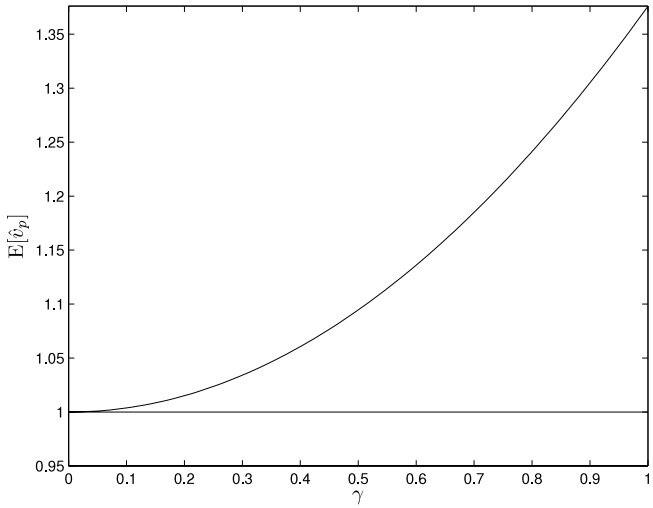

Fig. 2. Plot of canonical PARK estimator $\hat{v}_p(\gamma)$ mean value, as function of canonical drift γ. It is seen that with growth of γ PARK estimator becomes more and more biased. Straight line is the plot of canonical bridge $\hat{v}_b$, mean value.

4. Comparative efficiency of PARK and bridge estimators

Resting on analytical formulas for probability density functions (pdfs) of random variables (7) and (8), given in Appendix, we explore in this section some statistical properties of canonical PARK estimator $\hat{v}_p(\gamma)$ and the bridge one $\hat{v}_b$ (6).

Let us check, first of all, the unbiasedness of the canonical PARK estimator. To make it, let us calculate, with the help of pdf $q_x(\delta)$ (A.4), the mean square of oscillation $\mathrm{d} = h - l$ of the canonical Brownian motion $x(\tau, \gamma)$ at the zero canonical drift ($\gamma = 0$). After simple calculations we obtain

$$\mathbf{E}[\mathrm{d}^2] = 2 + \sum_{m=1}^{\infty} \frac{2}{m(4m^2 - 1)} = \ln 16.$$

From here and from expression (6) of canonical PARK estimator $\hat{v}_p(\gamma)$ one can see that the following expression is true

$$\mathbf{E}[\hat{v}_p(\gamma = 0)] = 1.$$

Let find now the factor κ at expressions (4) and (6). To do it, we calculate first of all the mean square of the bridge oscillation. Due to expression (A.5) for the bridge oscillation s (6) pdf, one has

$$\mathbf{E}[s^2] = \sum_{m=1}^{\infty} \frac{1}{m^2} = \frac{\pi^2}{6}.$$

Accordingly, the unbiased canonical bridge estimator has the form

$$\mathbf{E}[\hat{v}_b] = 1 \quad \Rightarrow \quad \kappa = 1/\mathbf{E}[s^2] \quad \Rightarrow \quad \hat{v}_b = 6\, s^2/\pi^2. \tag{10}$$

The great advantage of the bridge estimator is its unbiasedness for any drift. This remarkable property of the pointed out estimator is the consequence of the fact that the bridge $Z(t, t')$ (3) and its canonical counterpart $z(\tau)$ don't depend on the drift μ (canonical drift γ) at all. On the contrary, the PARK estimator becomes essentially biased at nonzero drift. In Fig. 2 the depicted dependence on γ of the canonical PARK estimator expected value illustrates the bias of the PARK estimator at nonzero drift. The corresponding curve is obtained with the help of analytical expression (A.3) for the canonical Brownian motion's oscillation d pdf.

Let calculate variances of the canonical PARK and bridge estimators. After substitution into the rhs of expression

$$\mathbf{E}[\hat{v}_p^2(\gamma = 0)] := \frac{1}{\ln^2 16} \int_0^{\infty} \delta^4 q_x(\delta) \mathrm{d}\delta$$

the sum (A.4) for the canonical Brownian motion oscillation pdf $q_x(\delta)$, and after summation we obtain for $\gamma = 0$:

$$\mathbf{E}[\hat{v}_p^2(\gamma = 0)] = 9\, \zeta(3)/\ln^2 16 \simeq 1.40733.$$

Accordingly, variance of canonical PARK estimator $\hat{v}_p$ is

$$\mathbf{Var}[\hat{v}_p(0)] = \frac{9\, \zeta(3)}{\ln^2 16} - 1 \simeq 0.407. \tag{11}$$

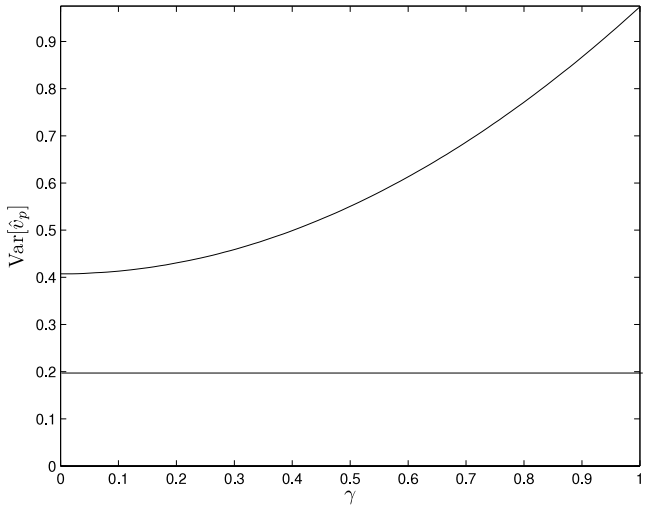

Fig. 3. Plots of dependence on γ of canonical PARK estimator variance. Straight line is the variance of canonical bridge estimator.

As the next step, we calculate variance of canonical bridge estimator $\hat{v}_b$ (10). The sought variance is equal to

$$\mathbf{Var}[\hat{v}_b] := \frac{36}{\pi^4}\,\mathbf{E}[s^4] - 1.$$

After substitution here, following from (A.5), the relation

$$\mathbf{E}[s^4] := \int_0^2 \delta^4 q_b(\delta)\mathrm{d}\delta = 3\sum_{m=1}^{\infty}\frac{1}{m^4} = \frac{\pi^4}{30},$$

obtains

$$\mathbf{Var}[\hat{v}_b] = \frac{6}{5} - 1 = 0.2. \tag{12}$$

Comparing equalities (11) and (12), one can see that variance of the bridge estimator is approximately twice as small than variance of the PARK estimator.

Recall that variance of the bridge estimator does not depend on drift. On the contrary, variance of the PARK estimator essentially depends on the drift. One can see it in Fig. 3, where a plot of dependence, on canonical drift γ, of the canonical PARK estimator variance is depicted.

Notice else that bias of some estimator is insignificant only if it is much smaller than the rms of the corresponding estimator, i.e. is smaller the relative bias:

$$\varrho := \frac{\mathbf{E}[\hat{v}(\gamma)] - 1}{\sqrt{\mathbf{Var}[\hat{v}(\gamma)]}}. \tag{13}$$

A plot of the canonical PARK estimator relative bias, as a function of canonical drift γ, is depicted in Fig. 4.

5. Interval estimations on the basis of PARK and bridge estimators

Given in Appendix analytical expressions (A.3), (A.4) and (A.5) for canonical Brownian motion and canonical bridge random oscillation pdfs allow us to explore in detail probabilistic properties of PARK and bridge canonical estimators. Let us find, at first, pdfs of the mentioned canonical estimator random values. It is well-known from Probabilistic Theory that pdf $W_p(x;\gamma)$ of the canonical PARK estimator is expressed through pdf $q_x(\delta;\gamma)$ (A.3) of the canonical Brownian motion oscillation by the relation

$$W_p(x;\gamma) = \sqrt{\frac{\alpha}{4x}}\,q_x\left(\sqrt{\alpha x};\gamma\right), \quad \alpha = \ln 16. \tag{14}$$

Similarly, pdf of the canonical bridge estimator is equal to

$$W_b(x) = \sqrt{\frac{\alpha}{4x}}\,q_b\left(\sqrt{\alpha x}\right), \quad \alpha = \frac{\pi^2}{6}. \tag{15}$$

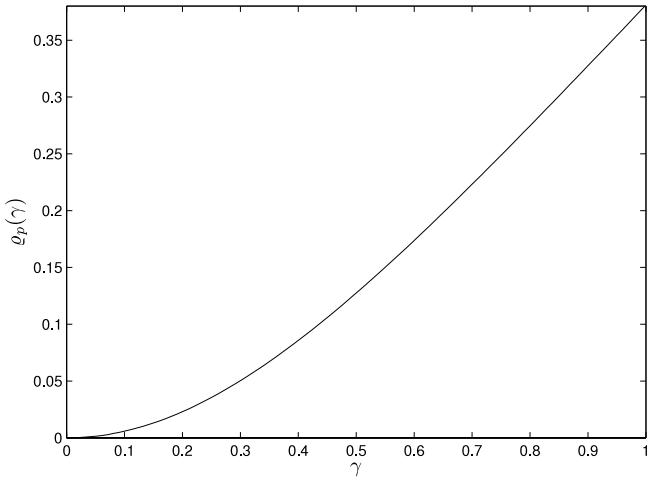

Fig. 4. Plot of relative bias (13) of canonical PARK estimator as function of canonical drift γ.

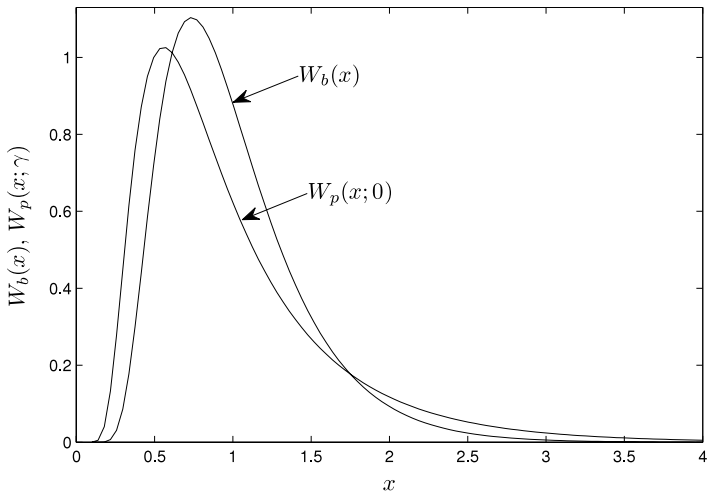

Fig. 5. Plots of canonical PARK and bridge estimators pdfs, clearly demonstrating "probabilistic preference" of bridge estimator in comparison with the PARK one.

Here $q_b(\delta)$ (A.5) is the pdf of the canonical bridge oscillation. Plots of the canonical PARK estimator pdf, for $\gamma = 0$, and pdf of the canonical bridge estimator are depicted in Fig. 5. In Fig. 6 are compared pdfs of the canonical PARK estimator, for $\gamma = 1$, and pdf of the canonical bridge estimator. It is seen in both figures that the pdf of the canonical bridge estimator is better concentrated around its expected value $\mathbf{E}[\hat{v}_b] = 1$ than the canonical PARK estimator pdf.

Knowing estimator pdfs, one can produce interval estimations of possible volatility values. Consider typical interval estimation. Let $\hat{V}$ be some volatility estimator, equal to

$$\hat{V} = V(T) \cdot \hat{v}. \tag{16}$$

Here $\hat{v}$ is the corresponding canonical estimator, while $V(T)$ is the measured volatility. One needs to find the probability

$$F(N) := \mathbf{Pr}\{V(T) < N \cdot \hat{V}\}$$

that the unknown (random) volatility $V(T)$ is not greater than N times the known (measured) volatility estimated value $\hat{V}$. It follows from (16) that the following inequalities are equivalent:

$$V(T) < N \cdot \hat{V} \quad \Leftrightarrow \quad \hat{v} > 1/N.$$

The last means in turn that the sought probability $F(N)$ is expressed through the pdf of canonical estimator $\hat{v}$ in the following way:

$$F(N) = \mathbf{Pr}\{\hat{v} > 1/N\} = \int_{1/N}^{\infty} W(x)\mathrm{d}x. \tag{17}$$

Here $W(x)$ is the pdf of canonical estimator $\hat{v}$.

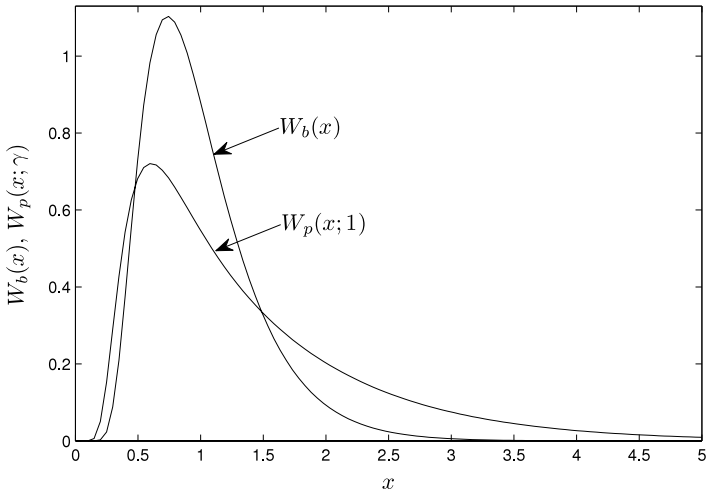

Fig. 6. Plots of PARK and bridge canonical estimators pdfs for $\gamma = 1$.

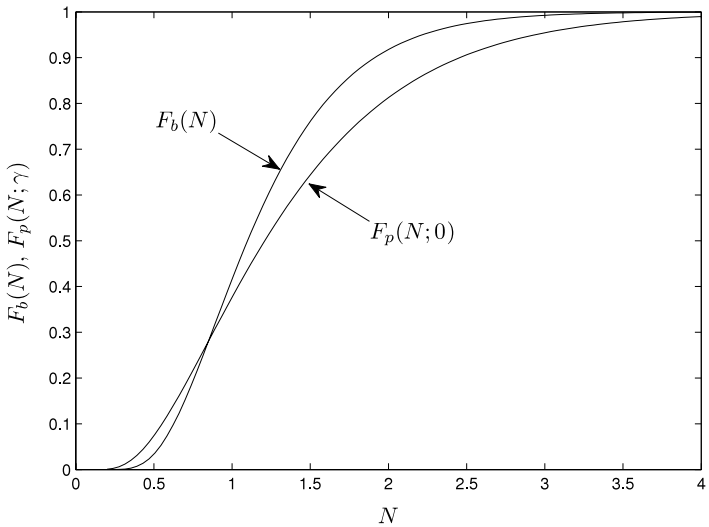

Fig. 7. Plots of probabilities $F_p(N)$ and $F_b(N)$ that true volatility is less than N times exceeding the values of PARK and bridge estimators.

Calculations, based on the relations (14), (15) and (17), give the result that the probability that the true volatility is less than twice the given bridge volatility estimator value $\hat{V}_b$ is equal to $F_b(2) = 0.918$. This is substantially larger than the analogous probability in the case of the PARK estimator: $F_p(2, \gamma = 0) \simeq 0.813$. The plots of the probabilities $F(N)$ (Eq. (17)) as a function of the level N, for the PARK estimator (in the case of zero drift $\mu = 0$) and for the bridge volatility estimator, are shown in Fig. 7.

6. Comparative statistics of canonical estimators

Above, we explored in detail statistical properties of the PARK and bridge estimators. Here we compare their statistics and statistics of other well-known volatility estimators: the GK and RS ones. Despite the previous sections, where we have used known analytical expressions for pdfs of canonical PARK and bridge estimators, below we use predominantly results of numerical simulations.

Namely, we produce $M \gg 1$ numerical simulations of random sequences

$$x_n(\gamma) := \gamma \frac{n}{N} + \frac{1}{\sqrt{N}} \sum_{n=1}^{N} \epsilon_n, \quad n = 0, 1, \ldots, N, \qquad x_0(\gamma) = 0, \tag{18}$$

where $\{\epsilon_n\}$ are iid Gaussian variables $\sim \mathcal{N}(0, 1)$. Notice that stochastic process $x_n(\gamma)$ of discrete argument n rather accurately approximates, for large $N \gg 1$, paths of canonical Brownian motion $x(\tau, \gamma)$ (5).

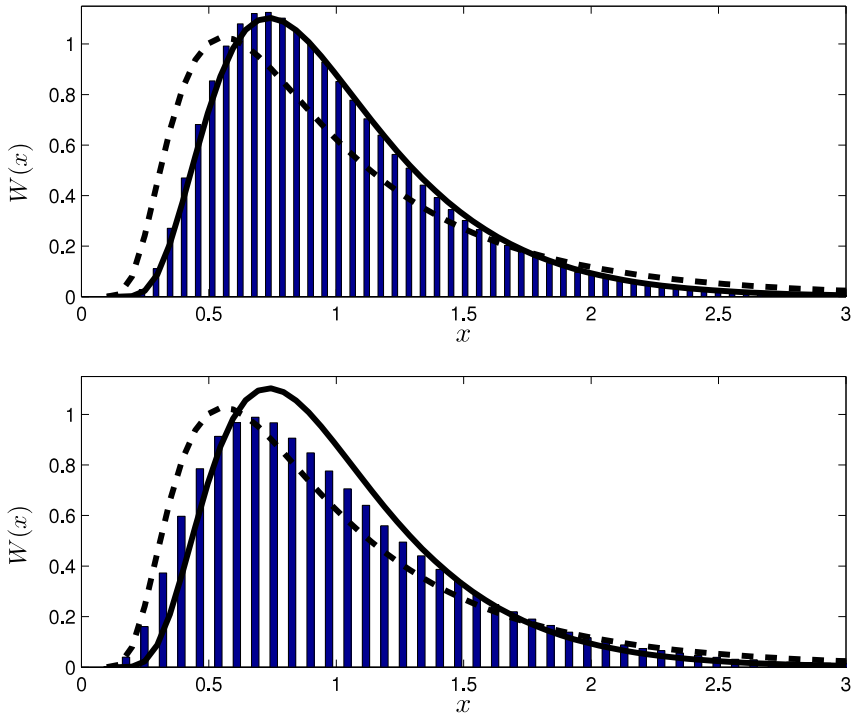

Fig. 8. *Upper panel.* Histogram of M samples of canonical bridge estimator $\hat{v}_b$. Solid line is the plot of canonical bridge estimator's pdf, given by analytical expression (15), and (A.5). Dashed line is the pdf of canonical PARK estimator for $\gamma = 0$. *Lower panel.* Histogram of M samples of canonical GK estimator $\hat{v}_g$ for $\gamma = 0$. Solid line is the plot of the canonical bridge estimator pdf. Dashed line is the canonical PARK estimator pdf for $\gamma = 0$.

Knowing M iid sequences $\{x_n(\gamma)\}$ one can find corresponding iid samples of the canonical estimators pointed out above. Everywhere below we take the number of iid samples M and discretization number N equal to

$$N = 5 \cdot 10^3, \qquad M = 5 \cdot 10^5.$$

Plots in Fig. 8 demonstrate rather convincingly the accuracy of numerical simulations. In Fig. 9 are given two hundred samples of canonical GK, RS, bridge and PARK estimators, ensuring "by the naked eye" that the canonical bridge estimator is more efficient than the GK one.

In Figs. 10 and 11 are given, obtained by numerical simulations, plots of canonical GK, PARK, RS and bridge estimators mean values and variances. These plots clearly demonstrate unbiasedness and high efficiency of the bridge estimator in comparison with the PARK, GK and RS estimators.

Finally, in Fig. 12 are shown the plots of probabilities that the true volatility $V(T)$ is larger than half the corresponding estimator value and less than twice it:

$$P_\Delta := \mathbf{Pr}\left\{\hat{V}/2 < V(T) < 2\hat{V}\right\} = \int_{1/2}^{2} W(x)\mathrm{d}x. \tag{19}$$

It is seen that for any γ the mentioned probability is essentially larger for the bridge estimator than for the GK, RS and PARK estimators.

Notice in conclusion that there are, in Figs. 10 and 12, some evident (but not essential) regular gaps between analytical curves and the results of numerical simulations. We suppose that the mentioned gaps are the consequences of the obvious discrepancy between, the comparatively regular, behavior of the process x_n (18) of discrete argument n and the wildly wrinkled dependence, on continuous time t, of the Brownian motion $B(t)$.

7. Conclusions

In this work we have analyzed statistical properties of the quadratic bridge volatility estimator, which is significantly more efficient than most, previously known, high–low-close volatility estimators.

Acknowledgments

For helpful and friendly comments we are grateful to all the referees. We are also grateful for scientific and financial support from the ETH (Zurich), Higher School of Economics (Russia, Nizhni Novgorod) and the Nizhni Novgorod State University (Russia).

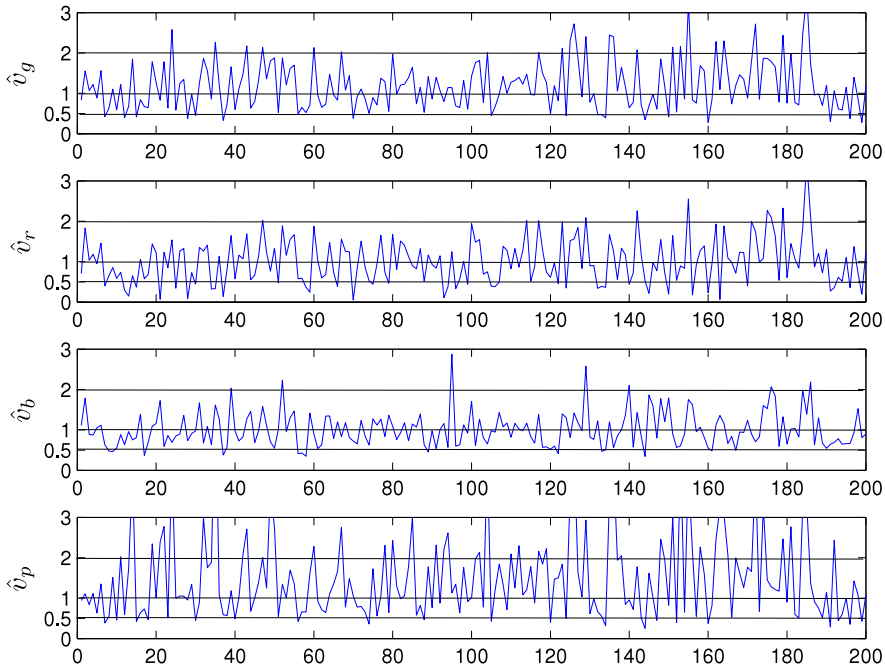

Fig. 9. Plots of two hundred samples of canonical estimators. Top to bottom are samples of GK, RS, bridge and PARK estimators. It is seen even by "the naked eye" that bridge estimator estimates volatility more accurately than the other mentioned estimators.

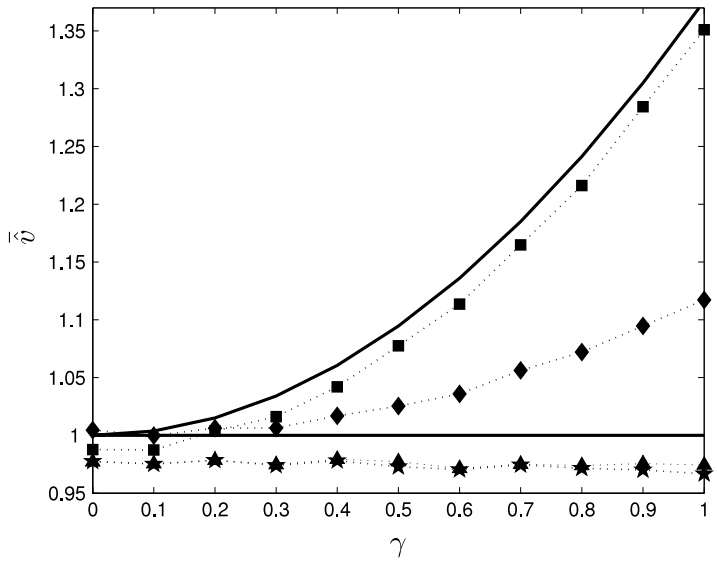

Fig. 10. Mean values $\bar{\hat{v}}$ of canonical PARK (■), GK (♦), RS (★) and bridge (▲) estimators. Solid lines are theoretical expectations, borrowing from Fig. 2.

Appendix A. Probabilistic properties of high, low and close values

Here are given pdfs of random variables (h, l, c) (7) and variables (ξ, ζ) (8), which one needs for canonical estimators (6) statistical analysis. Let us begin with random variable $c = x(1, \gamma)$. Obviously, its pdf is

$$f(\chi; \gamma) := \frac{1}{\sqrt{2\pi}} \exp\left(-\frac{(\chi - \gamma)^2}{2}\right), \quad \chi \in (-\infty, \infty).$$

It is easy to show, additionally, that joint pdf $q_x(\eta, \chi; \gamma)$ of high value h (7) of canonical Brownian motion $x(\tau, \gamma)$ and the close value $c = x(1, \gamma)$ is equal to

$$q_x(\eta, \chi; \gamma) = \sqrt{\frac{2}{\pi}}\,(2\eta - \chi)\,\mathrm{e}^{2\gamma\eta} \exp\left(-\frac{1}{2}(2\eta - x + \gamma)^2\right), \quad \chi < \eta,\ \eta > 0.$$

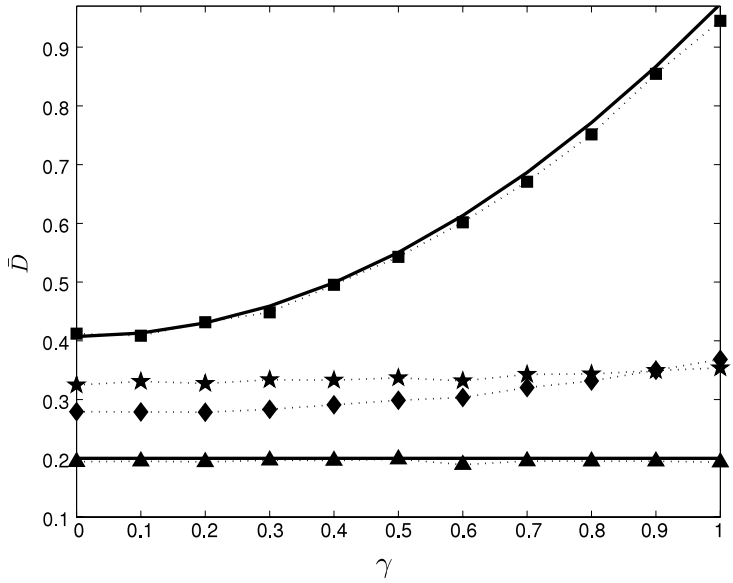

Fig. 11. Estimations $\bar{D}$ of variance of PARK (■), RS (★), GK (♦) and bridge (▲) canonical estimators. Solid lines are plots of theoretical variances, borrowed from Fig. 3. It is seen that for any γ bridge estimator's variance is significantly smaller than variances of other mentioned estimators.

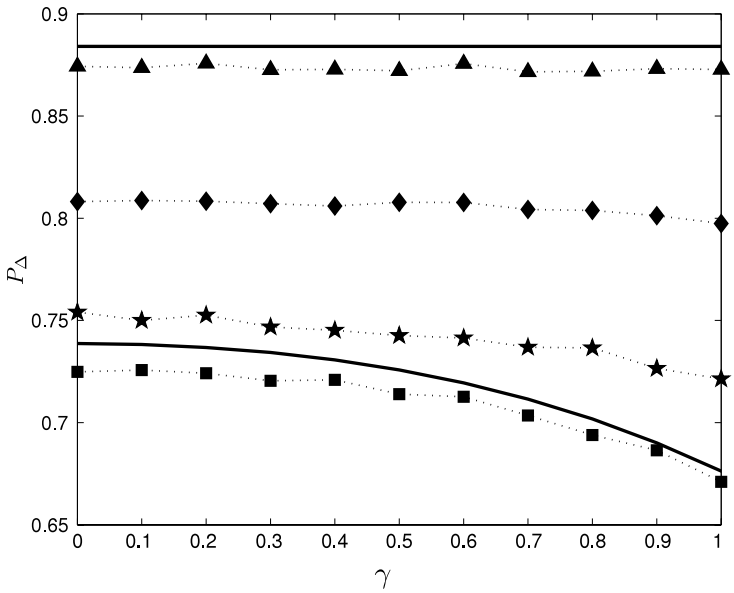

Fig. 12. Probabilities P_Δ (19) at different γ values for PARK (■), RS (★), GK (♦) and bridge (▲) estimators. Solid lines are results of theoretical calculations, resting on formula (19).

In turn, pdf of high value h (7)

$$q_x(\eta;\gamma) := \int_{-\infty}^{h} q_x(\eta,\chi;\gamma)\mathrm{d}\chi$$

is given by expression

$$q_x(\eta;\gamma) = \sqrt{\frac{2}{\pi}}\exp\left(-\frac{(\eta-\gamma)^2}{2}\right) - \gamma \mathrm{e}^{2\gamma\eta}\,\mathrm{erfc}\left(\frac{\eta+\gamma}{2}\right), \quad \eta > 0.$$

Let us write here an explicit expression for joint pdf $q_x(\eta,\ell,\chi;\gamma)$ of random variables (h, l, c) (7). Using formulas, given in the monograph [21] and in the article [22], one might show that the pointed out joint pdf is given by:

$$q_x(\eta,\ell,\chi;\gamma) = f(\chi;\gamma)\mathcal{S}(\eta,\ell|\chi),$$
$$\chi \in (\ell,\eta),\ h > \chi\mathbf{1}(\chi),\ \ell < \chi\mathbf{1}(-\chi). \tag{A.1}$$

Here $\mathbf{1}(\chi)$ is the unit step function, equal to unity for $\chi > 0$ and zero otherwise. Besides, above there is the function

$$\begin{aligned} \mathcal{S}(\eta, \ell|\chi) &:= \sum_{m=-\infty}^{\infty} m\left[m\mathcal{F}(m(\eta-\ell), \chi) + (1-m)\mathcal{F}(m(\eta-\ell)+\ell, \chi)\right], \\ \mathcal{F}(\eta, \chi) &:= \left[(\chi - 2\eta)^2 - 1\right] \mathrm{e}^{2\eta(\chi-\eta)}. \end{aligned} \tag{A.2}$$

To explore statistical properties of the canonical GK estimator, we need the joint pdf $q_x(\delta, \chi; \gamma)$ of canonical Brownian motion $x(\tau, \gamma)$ (5) oscillation $\mathrm{d} = h - l$ and the close value $c = x(1, \gamma)$. As it follows from (A.1), and (A.2), the mentioned pdf is equal to

$$\begin{aligned} q_x(\delta, \chi; \gamma) &= 4f(\chi; \gamma) \sum_{m=-\infty}^{\infty} m \times \left[m(\delta - |\chi|)[(|\chi| + 2m\delta)^2 - 1] - (m+1)(|\chi| + 2m\delta)\right] \mathrm{e}^{-2m\delta(|\chi|+m\delta)}, \\ &\delta > |\chi|, \ \chi \in (-\delta, \delta). \end{aligned}$$

After integration of above joint pdf over all χ values we obtain pdf $q_x(\delta; \gamma)$ of oscillation d:

$$\begin{aligned} q_x(\delta; \gamma) = 2 \sum_{m=-\infty}^{\infty} m\Bigg(&\sqrt{\frac{8}{\pi}} \mathrm{e}^{-\frac{\gamma^2}{2} - 2m^2\delta^2} \times \left[\mathrm{e}^{-\frac{\delta^2}{2}(1+4m)} \cosh(\delta\gamma)(1 + m(2+\gamma^2)) - m(2+\gamma^2)\right] \\ &+ \gamma\left[a(\delta, \gamma, m) + a(-\delta, \gamma, m)\right]\Bigg), \quad \delta > 0. \end{aligned} \tag{A.3}$$

Here we have used the auxiliary function

$$a(\delta, \gamma, m) := \mathrm{e}^{2m\delta\gamma}\left[1 + m(3 + \gamma(2m\delta + \gamma + \delta))\right] \times \left[\mathrm{erf}\left(\frac{2m\delta + \gamma + \delta}{\sqrt{2}}\right) - \mathrm{erf}\left(\frac{2m\delta + \gamma}{\sqrt{2}}\right)\right].$$

In the particular case of zero drift ($\gamma = 0$), one gets from (A.3) the following expression

$$q_x(\delta) = \sqrt{\frac{32}{\pi}} \sum_{m=-\infty}^{\infty} m\left[(1+2m)\mathrm{e}^{-\frac{(1+2m)^2\delta^2}{2}} - 2m\mathrm{e}^{-2m^2\delta^2}\right]. \tag{A.4}$$

All statistical properties of high and low values (8) of canonical bridge (9) are defined by their two-fold joint pdf $q_b(\eta, \ell)$, given by the relation

$$\begin{aligned} q_b(\eta, \ell) &= \sum_{m=-\infty}^{\infty} m\left[m\mathcal{F}(m(\eta-\ell)) + (1-m)\mathcal{F}(m(\eta-\ell)+\ell)\right], \\ \mathcal{F}(\eta) &:= 4(4\eta^2 - 1)\mathrm{e}^{-2\eta^2}. \end{aligned}$$

Following from here the pdf $q_b(\delta)$ of canonical bridge oscillation $s = \xi - \zeta$ is given by the equality

$$q_b(\delta) = 8\delta \sum_{m=1}^{\infty} m^2(4m^2\delta^2 - 3)\mathrm{e}^{-2m^2\delta^2}, \quad \delta > 0. \tag{A.5}$$

Appendix B. Probabilistic properties of high value and its instant

Consider random high value h (7) of canonical Brownian motion $x(\tau, \gamma)$ (5) and the random instant θ of the occurrence of this high is recorded:

$$\theta := h = x(\theta, \gamma).$$

Using formulas, given in the monograph [21] and in the article [22], one might show that the pointed out joint pdf $\phi(\eta, \vartheta; \gamma)$ of the mentioned pair of random variables (h, θ) is given by the expression:

$$\phi(\eta, \vartheta; \gamma) = \frac{\eta}{\vartheta\sqrt{\pi\vartheta}} \exp\left(-\frac{(\eta - \gamma\vartheta)^2}{2\vartheta}\right) \mathcal{V}(1-\vartheta, -\gamma), \quad \eta > 0, \ \vartheta \in (0, 1), \tag{B.1}$$

where

$$\mathcal{V}(\vartheta, \gamma) = \frac{1}{\sqrt{\pi\vartheta}} \exp\left(-\frac{\gamma^2\vartheta}{2}\right) + \frac{\gamma}{\sqrt{2}} \mathrm{erfc}\left(-\gamma\sqrt{\frac{\vartheta}{2}}\right).$$

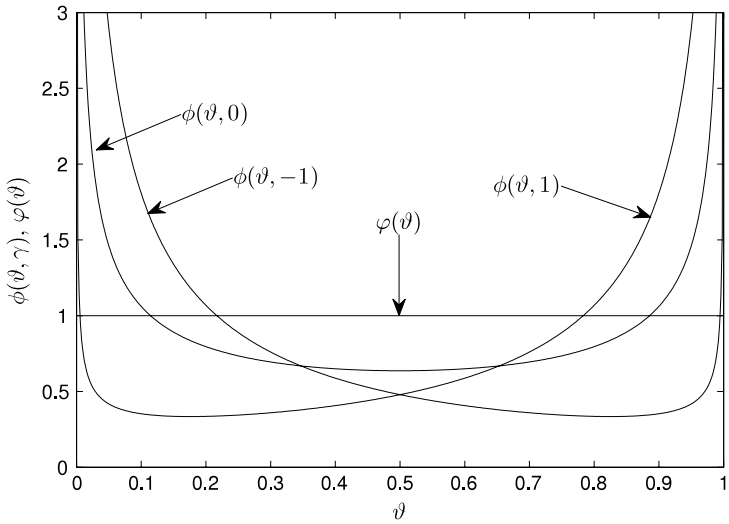

Fig. B.1. Typical plots of the canonical Brownian motion $x(\tau, \gamma)$ (5) high value occurrence instants pdf $\phi(\vartheta; \gamma)$ (B.2), for $\gamma = 0; \pm 1$, and corresponding uniform pdf $\varphi(\vartheta)$ (B.5) of the high value occurrence instances of the canonical bridge $z(\tau)$ (9).

After integration of joint pdf $\phi(\eta, \vartheta; \gamma)$ over the whole η values $\eta \in (0, 1)$, we obtain the pdf $\phi(\vartheta; \gamma)$ of the random instant θ of the high value occurrence:

$$\phi(\vartheta; \gamma) = \mathcal{V}(\vartheta, \gamma)\, \mathcal{V}(1 - \vartheta, -\gamma). \tag{B.2}$$

One can get an analogous pdf of the low value, replacing at the right hand side the last equality γ by $-\gamma$. In particular, in the case of zero drift ($\gamma = 0$) pdf (B.2) of the high (low) value occurrence reduces to the well-known arcsine distribution:

$$\phi(\vartheta; 0) = \frac{1}{\pi\sqrt{\vartheta(1 - \vartheta)}}. \tag{B.3}$$

Consider now the high value ξ (8) of the canonical bridge $z(\tau)$ (9) and the instant ρ of the high value occurrence:

$$\rho := \xi = z(\rho).$$

Joint pdf $\varphi(\eta, \vartheta)$ of the random variables (ξ, ρ) is well-known (see, for instance, Refs. [21,22]) and is equal to:

$$\varphi(\eta, \vartheta) = \sqrt{\frac{2}{\pi}}\, \frac{\eta^2}{\sqrt{\vartheta^3(1 - \vartheta)^3}}\, \exp\left(-\frac{\eta^2}{2\vartheta(1 - \vartheta)}\right), \quad \eta > 0,\ \vartheta \in (0, 1). \tag{B.4}$$

After integration of the last equality over all $\eta > 0$ values, we obtain the uniform distribution of the random instant ρ:

$$\varphi(\vartheta) = 1, \quad \vartheta \in (0, 1). \tag{B.5}$$

Plots of the pdf of the canonical Brownian motion high value occurrence $\phi(\vartheta; \gamma)$ (B.2) and uniform distribution (B.5) of the high (low) value of the canonical bridge occurrence are depicted in Fig. B.1.

References

[1] Y. Aït-Sahalia, P.A. Mykland, L. Zhang, How often to sample a continuous-time process in the presence of market microstructure noise, Rev. Financ. Stud. 18 (2005) 351–416.
[2] T.G. Andersen, T. Bollershev, F.X. Diebolt, P. Labys, Modeling and forecasting realized volatility, Econometrica 71 (2003) 529–626.
[3] D. Yang, Q. Zhang, Drift-independent volatility estimation based on high, low, open and close prices, J. Bus. 73 (2000) 477–491.
[4] F. Corsi, G. Zumbach, U. Müller, M. Dacorogna, Consistent high-precision volatility from high-frequency data, Econ. Notes 30 (2001) 183–204.
[5] T.G. Andersen, T. Bollershev, F.X. Diebolt, P. Labys, Modeling and forecasting realized volatility, Econometrica 71 (2003) 529–626.
[6] L. Zhang, P.A. Mykland, Y. Aït-Sahalia, A tale of two time scales: determining integrated volatility with noisy high-frequency data, J. Amer. Statist. Assoc. 100 (2005) 1394–1411.
[7] N. Kunitomo, Improving the Parkinson method of estimating security price volatilities, J. Bus. 65 (1992) 295–302.
[8] M. Parkinson, The extreme value method for estimating the variance of the rate of return, J. Bus. 53 (1980) 61–65.
[9] M. Garman, M.J. Klass, On the estimation of security price volatilities from historical data, J. Bus. 53 (1980) 67–78.
[10] L.C.G. Rogers, S.E. Satchell, Estimating variance from high, low and closing prices, Ann. Appl. Probab. 4 (1991) 504–512.
[11] L.C.G. Rogers, S.E. Satchell, Y. Yoon, Estimating the volatility of stock prices: a comparison of methods that use high and low prices, Appl. Financ. Econ. 4 (1994) 241–247.
[12] R.Y. Chou, N. Liu, The economic value of volatility timing using a range-based volatility model, J. Econom. Dynam. Control 34 (2010) 2288–2301.
[13] G. Ramey, V. Ramey, Cross-country evidence on the link between volatility and growth, Amer. Econ. Rev. 85 (1995) 1138–1151.
[14] G. Bonanno, D. Valenti, B. Spagnolo, Mean escape time in a system with stochastic volatility, Phys. Rev. E 75 (8) (2007) 016106.

[15] D. Valenti, B. Spagnolo, G. Bonanno, Hitting time distributions in financial markets, Physica A 382 (2007) 311–320.
[16] A. Saichev, D. Sornette, V. Filimonov, F. Corsi, Homogeneous volatility bridge estimators, Swiss Finance Institute Research Paper No. 09-46, Posted December 2009. http://ssrn.com/abstract=1523225.
[17] A. Saichev, D. Sornette, A simple microstructure return model explaining microstructure noise and Epps effects, Swiss Finance Institute Research Paper No. 12-08. http://ssrn.com/abstract=2009392.
[18] M. Jeanblanc, M. Yor, M. Chesney, Mathematical Methods for Financial Markets, Springer Verlag, London, 2009.
[19] R. Cont, P. Tankov, Financial Modelling with Jump Processes, CRC Press, London, 2004.
[20] A. Saichev, Ya. Malevergne, D. Sornette, Theory of Zipf's Law and Beyond, Springer Verlag, Heidelberg, 2010.
[21] A.N. Borodin, P. Salminen, Handbook of Brownian Motion—Facts and Formulae, second ed., Birkhäuser Verlag, Basel, 2002.
[22] A. Saichev, D. Sornette, Time-Bridge Estimators of Integrated Variance, 12 Aug 2011. arXiv:1108.2611v1 [q-fin.ST].